International Journal of Power Electronics and Drive System (IJPEDS)
Vol. 17, No. 1, March 2026, pp. 303~316
ISSN: 2088-8694, DOI: 10.11591/ijpeds.v17.i1.pp303-316

Mitigating harmonic distortion in grid-connected PV systems: a comparative evaluation of ANFIS and IC-based MPPT techniques

Bouledroua Adel, Mesbah Tarek, Kelaiaia Samia
Department of Electrical Engineering, Faculty of Technology, Badji Mokhtar University, Annaba, Algeria

Article Info

Article history:

Received Jul 15, 2025
Revised Dec 18, 2025
Accepted Jan 23, 2026

Keywords:

ANFIS
Incremental conductance
Maximum power point tracking
Power quality
Total harmonic distortion

ABSTRACT

Integrating photovoltaic (PV) systems into power grids presents notable challenges related to power quality, especially concerning total harmonic distortion (THD) caused by power electronic converters, which do not comply with IEEE 519 and IEC 61000 standards. This study introduces an adaptive neuro-fuzzy inference system (ANFIS)-based maximum power point tracking (MPPT) controller designed to optimize energy extraction while concurrently mitigating harmonic distortion in three-phase grid-connected PV systems. Unlike conventional IC-MPPT methods, which compromise the quality of the power to monitor performance, the proposed ANFIS-MPPT strategy uses intelligent modulation index adjustment to achieve a dual goal. A comparison of the four irradiation levels (450-1000 W/m²) shows a higher performance: ANFIS-MPPT achieves 0.26% THD at 1000 W/m² compared to 0.44% at IC-MPPT (40.9% improvement), and 0.80% versus 1.12% at 450 W/m² (28.6% reduction). The five-layer ANFIS architecture, trained on temperature and radiation data, shows faster convergence and lower oscillation than the conventional approach. The results confirm that MPPT based on ANFIS is an effective solution to improve the energy quality of grid-integrated photovoltaic installations while maintaining optimal energy conversion efficiency.

This is an open access article under the CC BY-SA license.

Corresponding Author:

Bouledroua Adel
Department of Electrical Engineering, Faculty of Technology, Badji Mokhtar University
Annaba 23000, Algeria
Email: adel.bouledroua@univ-annaba.dz

1. INTRODUCTION

Solar photovoltaic systems (PVs), as a clean and renewable source, have significantly changed the global energy landscape, with grid-connected installations achieving unparalleled levels worldwide [1], [2]. As these systems integrate into existing electrical grids, they serve as distributed generation sources that convert solar irradiance into electrical energy through power electronic converters. Though this integration raises serious power quality concerns, particularly harmonic distortion, which can undermine grid stability and contravene established power quality standards such as IEEE 519 and IEC 61000 [3], [4]. The non-linear characteristics of power electronic interfaces, combined with the inherent variability of solar irradiance and environmental conditions, create complex harmonic phenomena that require sophisticated mitigation strategies to ensure reliable grid operation [5], [6].

The basic challenge involves the dual objective of maximizing power extraction from photovoltaic (PV) arrays and maintaining an acceptable power quality standard. The maximum power point tracking (MPPT) technique is a key to optimizing solar power generation due to the continuous shifts of the MPP

caused by varying environmental conditions, including solar radiation, temperature, and partial shading [7], [8]. However, conventional MPPT algorithms often produce compromises between tracking efficiency and energy quality, especially under rapidly changing conditions [9], [10]. Harmonic distortion occurs due to the inherent switching functions of power electronics converters that play an important role in MPPT implementation. These distortions can be propagated in the electrical network, causing voltage distortions, energy loss, and potential interference with sensitive loads [11], [12]. This issue is further intensified by the simultaneous operation of multiple inverters in large-scale PV installations, which results in cumulative harmonic effects that exceed acceptable thresholds [13].

In the literature, several studies have been conducted on both MPPT optimization and harmonic mitigation approaches, but most studies focus on these topics separately rather than as interrelated challenges [6], [14], [15]. Conventional MPPT strategies such as P&O and IC are recognized for their straightforwardness and efficiency under stable conditions. However, they often exhibit oscillations around the MPP and face challenges in adapting to swiftly changing environmental conditions [16], [17]. In the recent advances in artificial intelligence, ANFISs for MPPT applications have been developed, which exhibit better tracking accuracy and faster convergence than traditional methods [18], [19]. Moreover, efforts towards power quality enhancement via active filtering techniques are also being made [20], [21], modified converter topologies [22], [23], and advanced control strategies [24]–[26] have been ongoing; yet, a comprehensive comparative assessment of how various MPPT schemes specifically affect harmonic distortion in grid-connected systems is limited in the literature.

This study proposes a novel comparative approach for the evaluation of the effectiveness of adaptive neuro-fuzzy inference system (ANFIS)-based and incremental conductance (IC)-based MPPT strategies, specifically in terms of total harmonic distortion (THD) mitigation in grid-tied PV systems. The developed simulation models that precisely represent the complex interactions between MPPT algorithms and harmonic generation mechanisms under varying levels of irradiance. The analysis employs MATLAB software's harmonic analysis tools to rigorously evaluate THD. The results show that ANFIS-MPPT methods consistently maintain a lower THD value and demonstrate the potential for a dual strategy for energy harvest and power quality. The study provides basic knowledge for energy system engineers and network operators and provides promising solutions to large-scale solar power plant deployments under strict power quality standards.

2. METHOD

2.1. System configuration and ANFIS-MPPT integration

Illustrated in Figure 1, the proposed grid-tied PV system operates in a three-phase, single-stage configuration and includes a PV array, a DC link capacitor, a three-phase voltage source inverter (VSI), an LCL filter, and the grid [19]. The PV array generates DC power that charges a DC link capacitor, forming the VSI input, where the variable irradiance and temperature must be considered, and it again stabilizes the DC bus voltage while attenuating a high-frequency ripple. The DC power is then converted into AC through a three-phase VSI synchronized to the grid through a phase-locked loop (PLL), whereby the LCL filter filters out the switching harmonics to meet the grid standards. The ANFIS-based MPPT controller was incorporated into the inverter closed-loop structure with a reconfigurable output, whereby the modulation index and switching signals were dynamically adjusted for simultaneous tracking of the MPP while satisfactorily regulating the harmonic distortion. The ANFIS algorithm uses real-time feedback from the PV array (voltage and current) and grid current harmonics to optimize the inverter pulse-width modulation (PWM) to keep the THD as low as possible while maximizing the MPPT efficiency. The proposed model has been simulated with MATLAB Simulink software, which allows for a comprehensive analysis and visualization of the behavior of the system. Detailed specifications and parameters of the components used in the simulation are given in Table 1 in order to ensure that the results are clear and reproducible.

2.2. PV array modelling

Modelling PV cells is essential for understanding and optimizing solar energy systems. The single-diode model (SDM) is the dominant approach for simulating their electrical behavior [27]. In Figure 2, the SDM treats a photovoltaic cell as an equivalent circuit consisting of a current source, a diode, and resistors. The current source generates photocurrent (I_{ph}) directly proportional to the intensity of the incident solar light and the cell area. The diode is modeled as a p-n junction, which accounts for the cell's nonlinear current-voltage properties. The circuit includes a series resistance (R_s) representing material and contact resistance, and a shunt resistance (R_{sh}) accounting for leakage currents [28]. This equivalent circuit simplifies the analysis of the performance of PV cells under different conditions and thus enables design optimization and efficiency improvements. The fundamental equation describing the model's current-voltage (I-V) characteristic is given as (1) [29], [30].

$$I = I_{ph} - I_d - \frac{(V+IR_S)}{R_{sh}} \quad (1)$$

Where I and V are the output current and voltage, respectively. The diode current I_d is calculated using the Shockley diode (2).

$$I_d = I_0(e^{\frac{(V+IR_S)}{nV_T}} - 1) \quad (2)$$

Here, I_0 is the reverse saturation current, and n is the diode ideality factor. The thermal voltage V_T is defined by (3).

$$V_T = \frac{kT}{q} \quad (3)$$

In (3) k is the Boltzmann constant (1.38×10^{-23}J/K), T is the absolute temperature, and q is the charge of an electron (1.602×10^{-19}C). In this context, I_0 is the reverse saturation current, n is the ideality factor of the diode, V_T is the thermal voltage, k is the Boltzmann constant (1.38×10^{-23} J/K), T is the absolute temperature, and q is the charge of an electron (1.602×10^{-19} C).

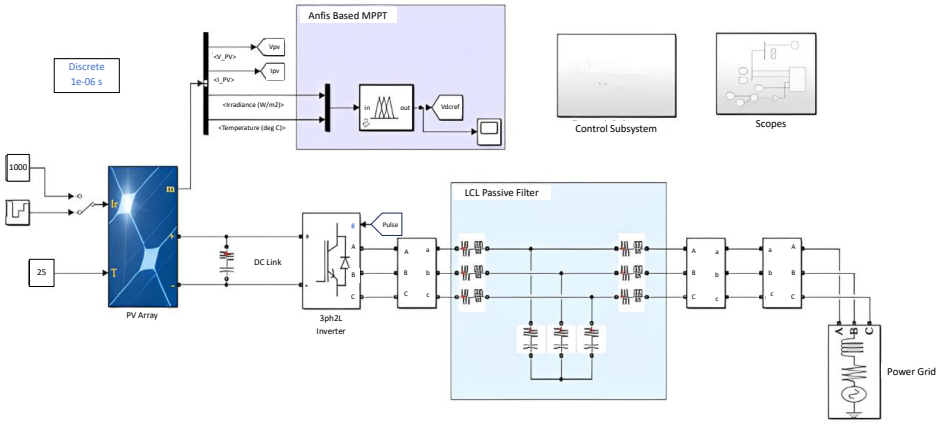

Figure 1. Proposed PV system

Table 1. Specifications values for the proposed model

Specifications	Value
PV array's rated power (P_{pv})	102 Kw
Open-circuit voltage of the PV array (V_{oc})	907.6 V
Capacitor of DC-link (C_{dc})	1000 µF
Switching frequency (F_{sw})	10 Khz
LCL filter inductor on the inverter side (L_i)	500 µH
LCL filter capacitor (C_f)	100 µF
LCL filter inductor on the grid side (L_g)	500 µH
Line to line grid voltage (V_{LL})	400 V
Frequency of the grid (f_g)	50 Hz

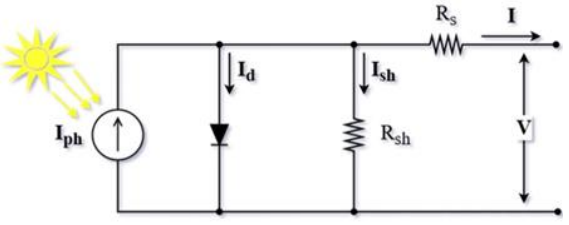

Figure 2. Single diode model of PV cell

Figure 3 shows the characteristics curves of current (I-V) and current (P-V) voltages in photovoltaic modules at different levels of solar radiation. Figure 3(a) shows an I-V curve corresponding to a radiation level of 1000, 750, 500, and 250 W/m^2, indicating that as the radiation increases, the short circuit current increases to a maximum value of 1000 W/m^2. The direct connection between solar radiation and PV module output current has been observed. Figure 3(b) shows the P-V curve that is equivalent, and the radiation controls the voltage level of the peak of the output. In particular, as the radiation increases, the power production increases, and the curve of 1000 W/m^2 shows the highest peak power, followed by other levels in the declining order. These data highlight the need for efficient MPPT methods to maximize energy recovery in changing environmental conditions and highlight the significant part of solar radiation used to select the efficiency and performance of solar systems [31]. test it and assess the effects of radiation and temperature under different environmental conditions.

Figure 4 shows the impact of temperature changes on the I-V and P-V characteristics curves of PV modules. Figure 4(a) presents the I–V curves at four different temperatures: 15 °C, 25 °C, 35 °C, and 45 °C. When the temperature rises, short circuit current remains relatively stable, open circuit voltage decreases, and overall curves are moved to lower voltages at higher temperatures. This behavior indicates that high temperatures may have a negative impact on the voltage output of PV modules. Figure 4(b) is the corresponding P-V curve and highlights the MPPs of each temperature condition. Optimal output is attained at the minimum voltage and a temperature of 25 °C. Optimum output is achieved with a minimum voltage and a temperature of 25 °C. However, as temperatures rise above that threshold, the maximum power falls significantly. This situation highlights the crucial role of temperature management in PV systems, as excessive heat can significantly reduce efficiency and overall energy production. The introduction of efficient cooling methods is therefore essential to increase performance under different temperature conditions [32].

This study investigates the power output capabilities of the SunPower SPR-215-WHT-U PV module, configured with 19 series-connected modules per string and 25 parallel strings, resulting in a total power capacity of up to 102 kW. Detailed parameters of the PV module are presented in Table 2, which supports the analysis of its performance characteristics.

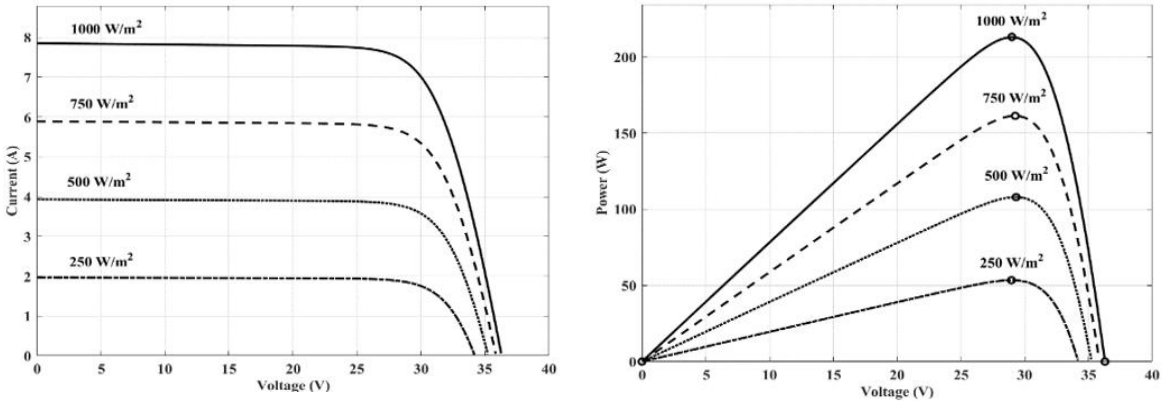

(a) (b)

Figure 3. Effect of solar irradiance on (a) I-V characteristics curve and (b) P-V characteristics curve

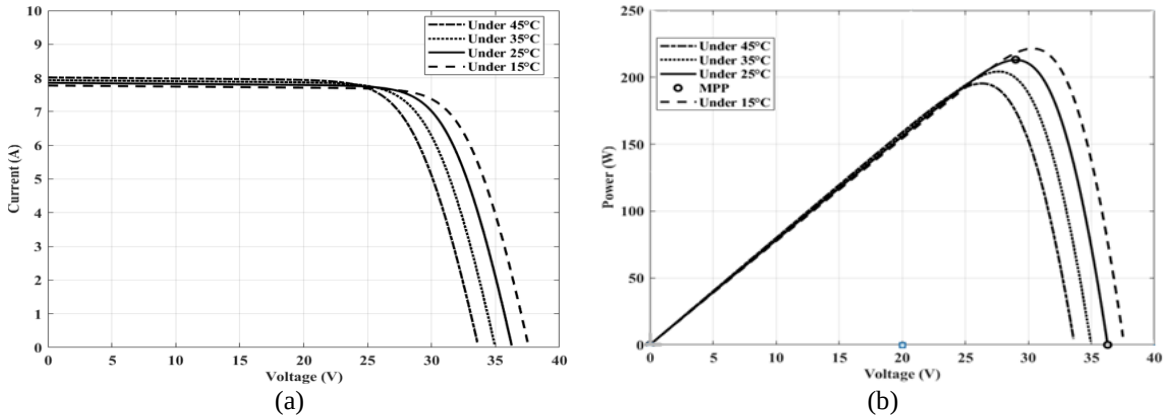

(a) (b)

Figure 4. Effect of temperature on (a) I-V characteristics curve and (b) P-V characteristics curve

Table 2. SunPower SPR-215-WHT-U PV module specification

Specification	Value
Maximum power P_{MP} (W)	214.92
Open circuit voltage V_{oc} (V)	48.3
Voltage at MPP V_{MP} (V)	39.8
Short-circuit current I_{sc}(A)	5.8
Current at MPP I_{MP} (A)	5.4
Temperature coefficient of V_{oc} (%/deg.C)	-0.27917
Temperature coefficient of I_{sc} (%/deg.C)	0.035897

2.3. MPPT approaches

MPPT is a critical function in PV systems, enabling optimal energy extraction under dynamic environmental conditions such as varying solar irradiance and temperature [33]. It maximizes energy gathering, improves general system efficiency, and raises PV installation return on investment. MPPT works by constantly tracking the solar panel voltage and current and adjusting the electrical operating point to extract most of the power. The system identifies and maintains the maximum power point (MPP) through an algorithm that is able to adjust the MPP according to solar irradiance, ambient temperature, and the characteristics of the photovoltaic panels [34]. MPPT guarantees increased battery life in off-grid systems, thus reducing the energy loss from photovoltaic systems and ensuring that solar panels perform best in different weather conditions [35].

2.3.1. IC MPPT technique

Incremental conductance (IC) is a widely used MPPT technique used in PV systems to address the non-linear power output and operating voltage dynamics of solar panels under varying environmental conditions [36], [37]. IC is often favored over heuristic methods like perturb and observe (P&O) because it uses analytical current and voltage derivatives to accurately pinpoint the MPP, where the P-V slope (dP/dV) reaches zero [36]. Through this technique, the system reduces steady-state power oscillations around the MPP while efficiently maintaining a fast response to swift changes in irradiance and temperature [38].

The IC MPPT flowchart, illustrated in Figure 5, outlines a structured process for dynamically adjusting the reference voltage V_{ref} to achieve optimal power extraction. The control system begins by acquiring measurements of the PV system's voltage V(k) and current I(k) at the current step and then calculates the incremental changes in voltage (ΔV) and current (ΔI) using (4) and (5) [39], [40].

$$\Delta V = V(k) - V(k-1) \tag{4}$$

$$\Delta I = I(k) - I(k-1) \tag{5}$$

If ΔV is zero, indicating no voltage change, the algorithm checks if:

$$I + \left(\frac{\Delta I}{\Delta V}\right) = 0 \tag{6}$$

This condition signifies that the MPP has been reached, and the system maintains the current reference voltage. If the MPP has not been reached, the flowchart evaluates the sign of the derivative term:

$$I + \left(\frac{\Delta I}{\Delta V}\right) > 0 \tag{7}$$

The operating point is to the left of the MPP, necessitating an increase in Vref to shift toward the maximum power point. Conversely, if:

$$I + \left(\frac{\Delta I}{\Delta V}\right) < 0 \tag{8}$$

The system must decrease Vref to move directly to the MPP. This iterative process continues until the optimal voltage is achieved, maximizing energy yield and boosting the PV system's efficiency. The (6) serves as the core criterion for determining the necessary adjustments to Vref based on the incremental changes in current and voltage.

2.3.2. ANFIS-MPPT approach

ANFIS is a high-level computational intelligence technique that synergizes language processing and fuzzy logic capabilities with the learning and adaptation mechanisms of artificial neural networks [39], [41]. This hybrid architecture allows ANFIS to model complex nonlinear input-output relationships by means of a systematic learning process, which makes it particularly suited for MPT applications where the optimal operating point is highly nonlinear in relation to a number of environmental variables. ANFIS uses historical data to learn the complex mapping between environmental conditions (temperature and irradiance) and the corresponding optimal voltage that yields maximum power extraction, in contrast to traditional MPPT algorithms that rely on instantaneous measurements and predetermined decision rules.

The development of the ANFIS-based MPPT controller necessitates robust datasets that encapsulate the nonlinear relationship between environmental variables and the photovoltaic (PV) system's MPP [42]. To achieve this, simulation-based data generation was employed, leveraging the single-diode model of the PV module, which incorporates temperature-dependent current and voltage coefficients Ki and Kv to replicate real-world operational dynamics. The photocurrent I_{ph} and open-circuit voltage V_{oc} were adjusted using Ki

and Kv, respectively, to account for temperature variations T, while irradiance G scales the photocurrent proportionally. By systematically varying G (0–1000 W/m²) and T (15–45 °C), the I-V characteristics were numerically solved to extract V_{mpp} and I_{mpp}, generating a comprehensive dataset that reflects the PV array's response to dynamic conditions. The (9) and (10) is used to calculate V_{mpp} and I_{mpp} [42].

$$I_{mpp} = \left(I_{SC,STC} + K_i(T - T_{STC})\right).\frac{G}{G_{STC}} \quad (9)$$

$$V_{mpp} = V_{oc,STC} + K_v(T - T_{STC}) \quad (10)$$

The standard test conditions (STC) subscript represents the standard test conditions (GSTC = 1000 W/m², TSTC = 25 °C), Ki represents the current temperature coefficient (A/°C), Kv represents the voltage temperature coefficient (V/°C).

The ANFIS architecture, illustrated in Figure 6, takes this simulated normalized data set as its primary input, so that the fuzzy inference system can use the implicit correlations between environmental inputs and optimal voltage as output. The approach helps to train the ANFIS controller on physically accurate worst-case scenarios such as rapid irradiance transients and thermal gradients, and is well prepared to reduce harmonic distortion while maintaining MPPT efficacy in grid-connected systems. The ANFIS-based MPPT in this work uses a five-layer architecture to map irradiance G and temperature T inputs to the optimal voltage V_{mpp} output. Layer 1 (fuzzification) is a representation of linguistic variables in which membership functions are used to transform crisp inputs into fuzzy sets. Layer 2 (rule) uses fuzzy logic principles to determine the firing force of a predefined IF-THEN rule. Layer 3 (normalization) scales these firing forces to ensure that their total sum is the same as unity, thereby reducing the ambiguity of the rule weight. Layer 4 (defuzzing) uses linear functions to calculate the corresponding parameters of each rule. In the final stage, Layer 5 (summation) combines the weighted results from Layer 4 to yield a precise Vmpp value, enabling accurate regulation in changing environmental conditions. This hybrid structure uses neural networks to adaptively learn membership functions, and uses fuzzy logic to interpret rules-based decision-making, thus achieving high performance of MPPT for different irradiations.

The structure was designed to convert solar irradiation and temperature into three appropriate membership functions (MFs), as illustrated in Figures 7 and 8. The shape of these MFs generated by the ANFIS controller evolves throughout the training phase. The forms of the MFs were obtained during and at the conclusion of the training phase.

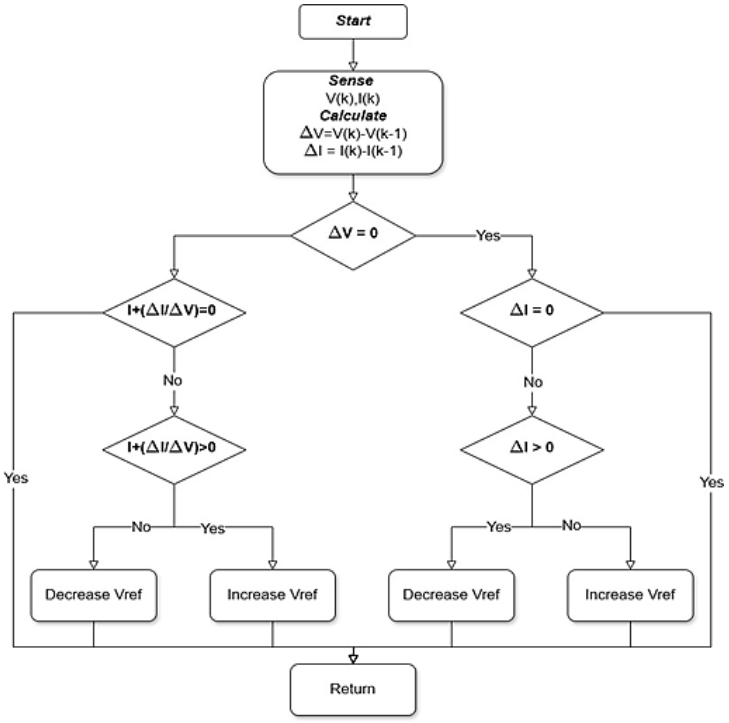

Figure 5. Flowchart of IC algorithm

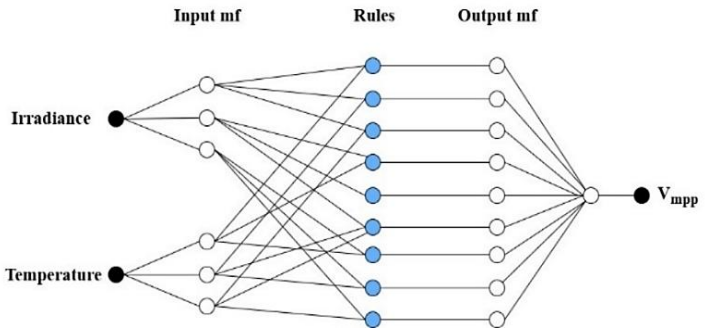

Figure 6. ANFIS-based MPPT structure

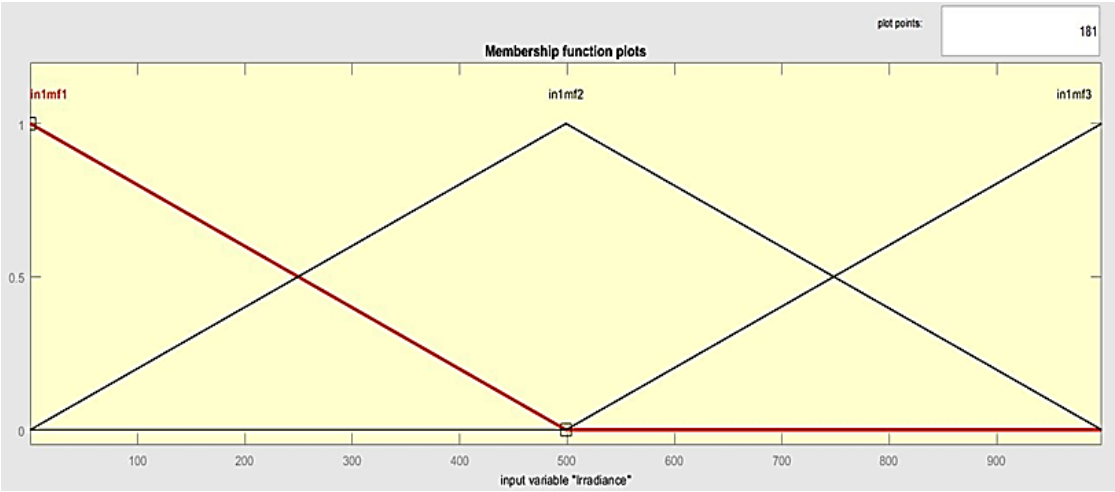

Figure 7. Irradiance input MF

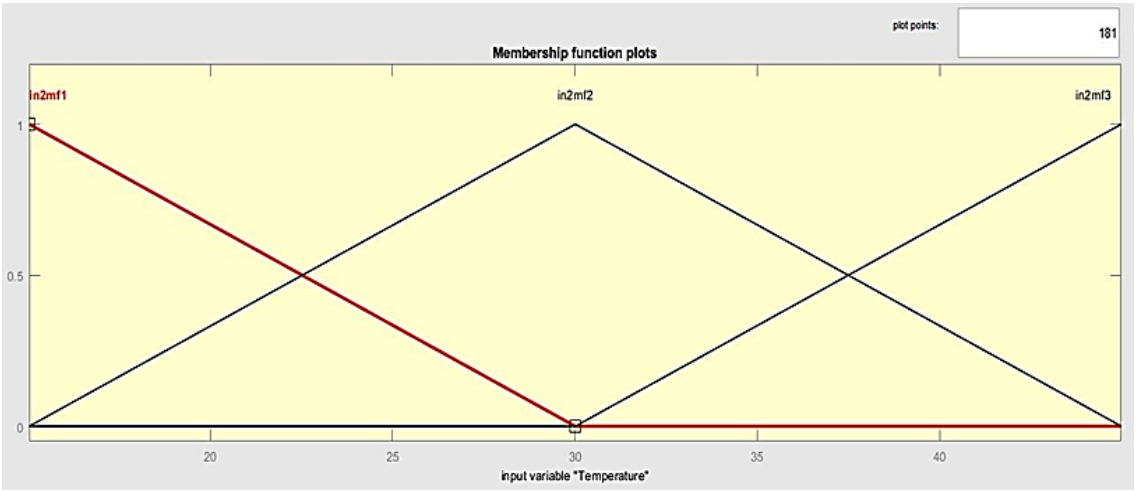

Figure 8. Temperature input MF

Figure 9 graphically depicts the fuzzy rules for a temperature of 23 °C and solar irradiation of 650 W/m², illustrating the relationships and correlations between the variables. All conditions can be adjusted by manipulating the slider on the graph. As indicated in the final column, the temperature ranges from 15 °C to 45 °C, solar irradiation varies between 0 and 1000 W/m², and the MPP voltage changes accordingly.

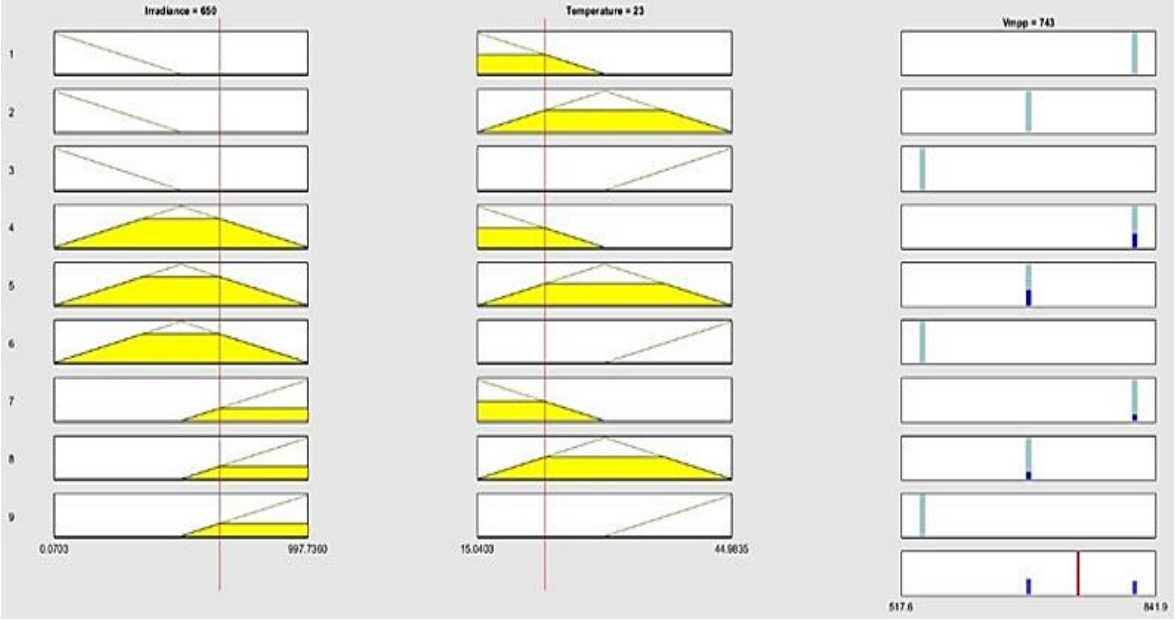

Figure 9. The fuzzy rules surface of ANFIS controller

3. RESULTS AND DISCUSSION

The dynamic irradiance profile used in this study, as shown in Figure 10, was meticulously crafted to replicate real-world solar variability and rigorously evaluate the performance of the proposed ANFIS-based MPPT controller. The profile encompasses a 1.35-second simulation interval, characterized by abrupt fluctuations and transitions between 450 W/m² and 1000 W/m² irradiation levels. These variations were deliberately structured to simulate transitional environmental conditions such as sudden cloud cover and rapid solar intensity changes, challenging the stability and responsiveness of grid tied PV systems in practical applications. The graph shows a sharp gradient of 0.35, 0.7, and 1.05 seconds, simulated in extreme scenarios, and validates the controller's ability to maintain MPPT efficiency and suppress harmonic distortion. This profile ensures comprehensive testing of the adaptability of the ANFIS model, highlighting its ability to recalibrate power extraction strategies under discontinuous solar input swiftly. This experimental setup aligns with the study's objective of evaluating THD mitigation and energy yield optimization in grid-tied systems subjected to unpredictable irradiation dynamics. Table 1 summarizes the key parameters of the model proposed in Figure 1.

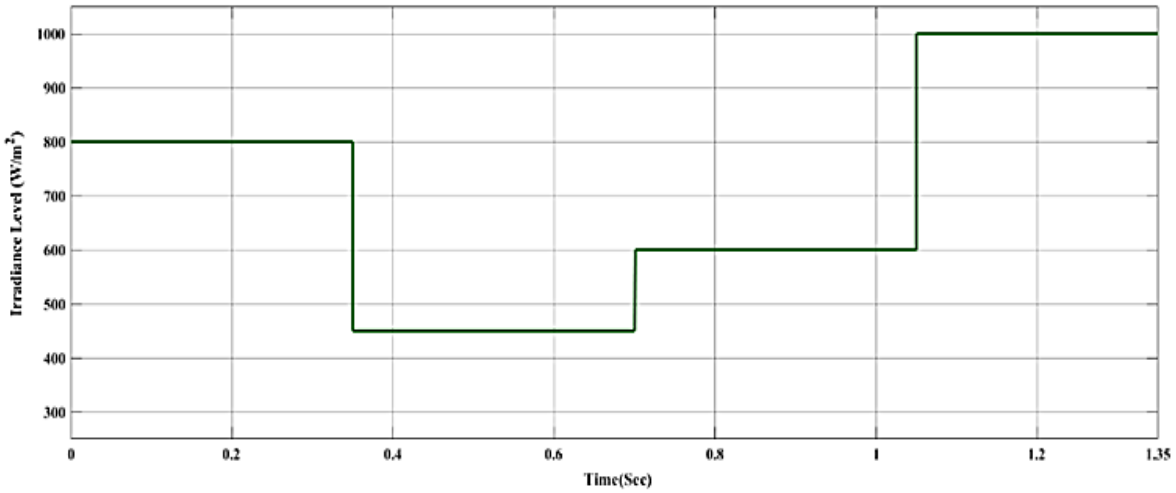

Figure 10. Irradiance profile

3.1. THD analysis

3.1.1. THD analysis at 800

The performance of MPPT techniques at an irradiance level of 800 W/m^2 is detailed in Figure 11, which presents the harmonic spectrum plots for both control strategies, fulfilling the requirement for visualization of the harmonic content. Under this condition, the ANFIS-based MPPT strategy (Figure 11(a)) achieved a THD value of 0.38%. On the other hand, the conventional incremental conductance (IC-MPPT) technique (Figure 11(b)) produced a higher THD of 0.65%. This variation highlights the ANFIS method's exceptional capability in reducing harmonic distortion. The visualization of the harmonic spectrum demonstrates that the adaptive ANFIS controller effectively diminishes the magnitude of specific lower-order harmonics resulting from the switching behavior of the VSI.

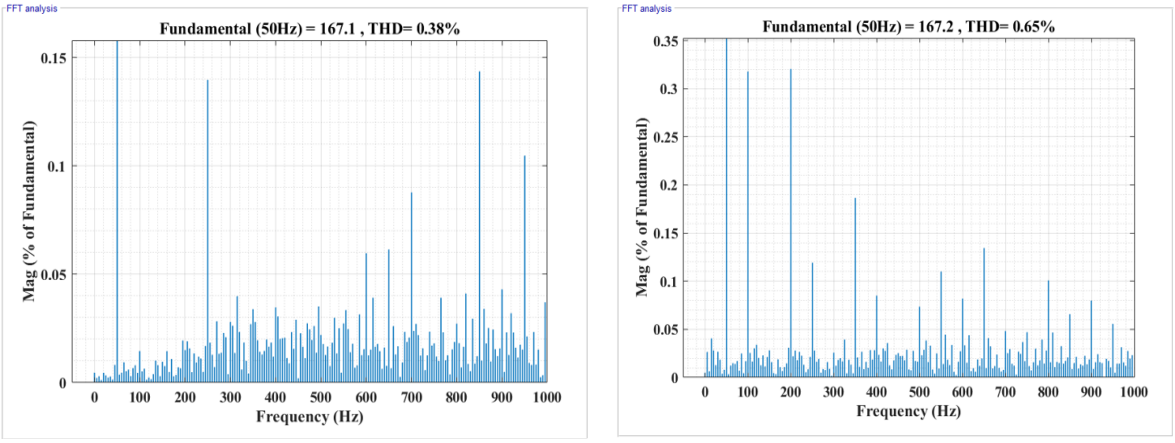

(a) (b)

Figure 11. THD analysis at 800 W/m^2: (a) ANFIS-MPPT and (b) IC-MPPT

3.1.2. THD analysis at 450

Figure 12 provides a comparative THD analysis at the lower irradiance level of 450 W/m², a scenario that rigorously challenges the adaptability of the MPPT controllers under less-than-optimal solar conditions. Figure 12(a) shows the THD profile of the ANFIS-MPPT strategy, which registers a THD of 0.80%. This relatively low distortion indicates the ability of the ANFIS controller to effectively mitigate harmonic distortion and thus improve the quality of the power output even under lower solar irradiance conditions. Conversely, Figure 12(b) illustrates the IC-MPPT approach, which exhibited a substantially higher THD of 1.12%. The visualization of the harmonic spectrum plots (Figure 12) confirms that the ANFIS method significantly suppresses the propagation of harmonics into the grid compared to the IC method.

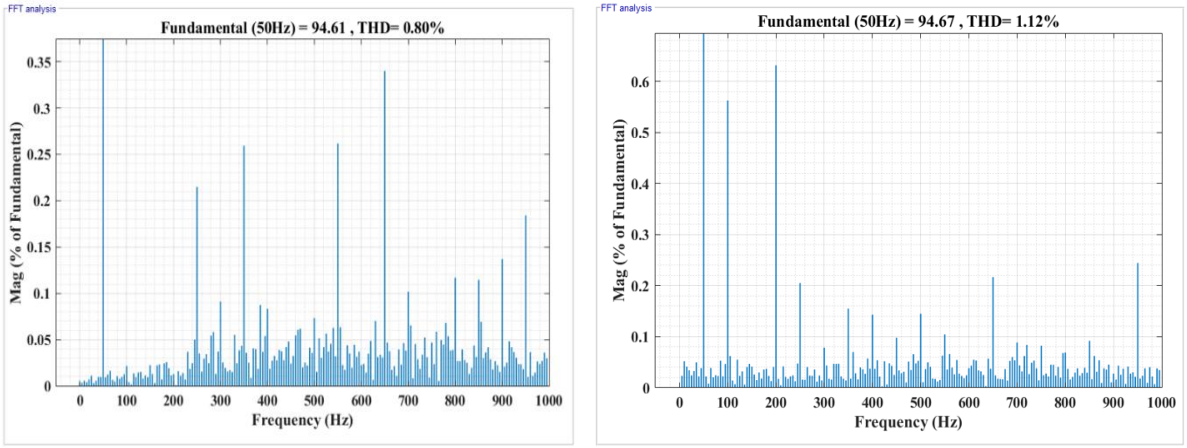

(a) (b)

Figure 12. THD analysis at 450 W/m^2: (a) ANFIS-MPPT and (b) IC-MPPT

3.1.3. THD analysis at 600

Figure 13 shows the harmonic spectrum analysis carried out at a 600 W/m^2 radiation level and provides important details on the control capabilities of the two MPPT strategies. Figure 13(a) specifically focuses on the THD profile of the MPPT method based on ANFIS, which recorded a THD of 0.56 %. This value demonstrates the consistent effectiveness of ANFIS in maintaining a low distortion rate, even as the irradiance drops from STC. Conversely, Figure 13(b) shows that the IC-MPPT method yielded a significantly higher THD of 0.86%. The increased harmonic distortion associated with the IC approach indicates its diminished effectiveness in harmonic management compared to ANFIS under this condition. By maintaining a THD 35% lower than that obtained by the IC method at 600 W/m^2.

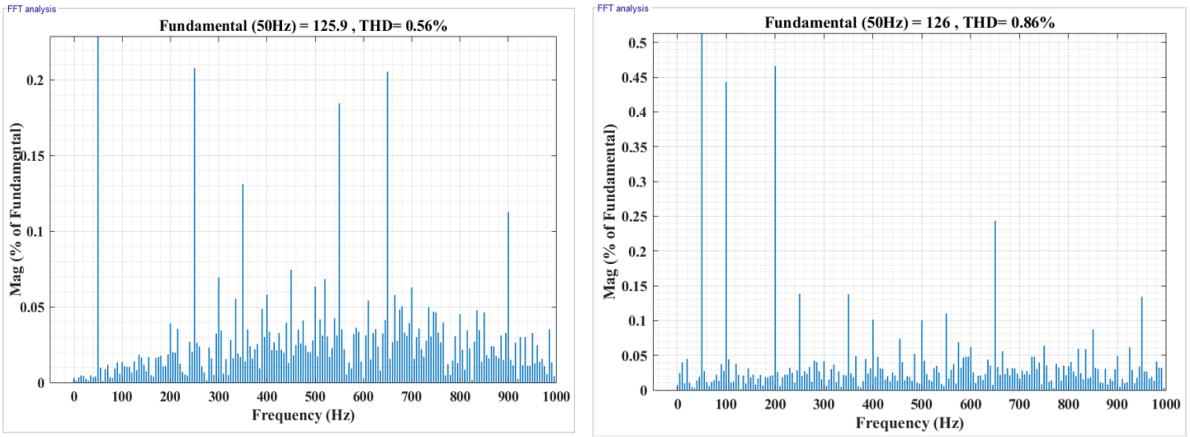

(a) (b)

Figure 13. THD analysis at 600 W/m^2: (a) ANFIS-MPPT and (b) IC-MPPT

3.1.4. THD analysis at 1000

The results depicted in Figure 14 provide a comparative THD analysis under standard test conditions (STC), specifically at an irradiance level of 1000 W/m² and a temperature of 25 °C. Figure 14(a) shows the harmonic spectrum visualization for the ANFIS-based MPPT method with a THD of 0.26%. This outcome is crucial, as attaining THD below 0.3% under STC indicates excellent power quality, strongly supporting the capability of the ANFIS strategy for harmonic suppression. In contrast, Figure 14(b) represents the incremental conductance (IC-MPPT) technique, which shows THD of 0.44%. This increase in THD suggests that the conventional IC method is significantly less adept at harmonic reduction than the intelligent ANFIS model, even under optimal environmental conditions. The ANFIS approach delivers a THD that is approximately 41% lower than the IC method at 1000 W/m². The superior performance positions the ANFIS-MPPT as a promising solution for the integration of photovoltaic systems into power grids.

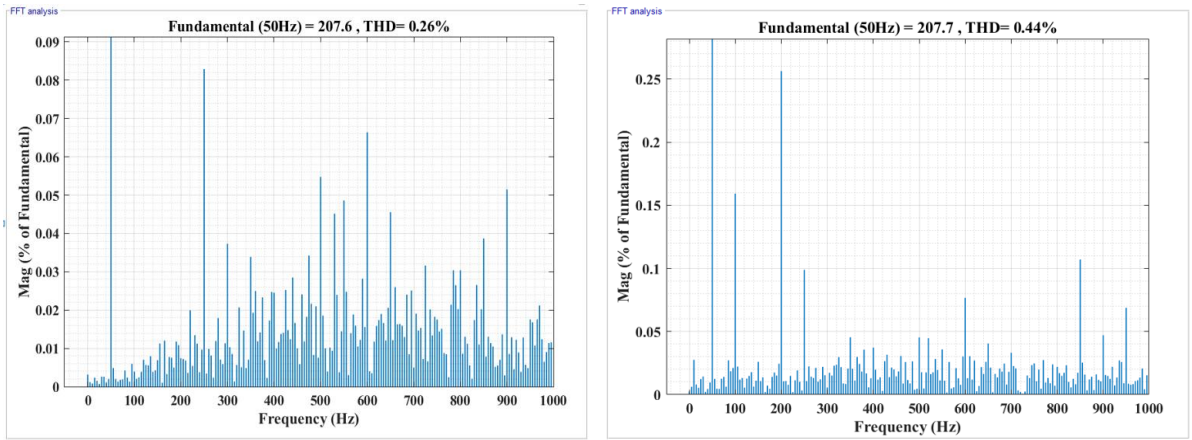

(a) (b)

Figure 14. THD analysis at 1000 W/m^2: (a) ANFIS-MPPT and (b) IC-MPPT

3.2. Injected current waveform to power grid

Figure 15 illustrates that the ANFIS-based MPPT controller exhibits superior dynamic performance by rapidly adjusting the amplitude of the grid current injected in response to abrupt changes in solar irradiance from 450 to 1000 W/m^2. Significantly, the enlarged viewports verify that the output current consistently exhibits a smooth and high-quality sinusoidal waveform across all operating conditions, thereby minimizing harmonic distortion despite sudden environmental changes. This behavior shows that controllers can ensure stable grid integration and strict compliance with energy quality standards, even when photovoltaic power generation transitions.

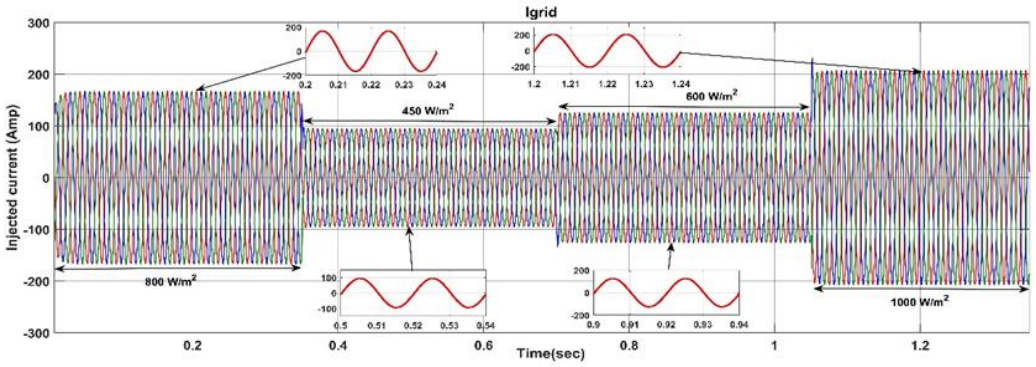

Figure 15. Three-phase injected grid current under varying solar irradiance levels using ANFIS-MPPT

As shown in Figure 16, the IC-MPPT controller is effective in regulating the amplitude of the injected grid current in direct correlation to the step changes in solar irradiance (450-1000 W/m^2), which demonstrates the reliable performance of the monitoring. The magnified insets confirm that the current waveform remains sinusoidal at all irradiation levels. This maintenance of waveform quality under temporary conditions underlines the ability of the IC algorithm to provide low overall harmonic distortion and to ensure a stable supply of energy to the power grid.

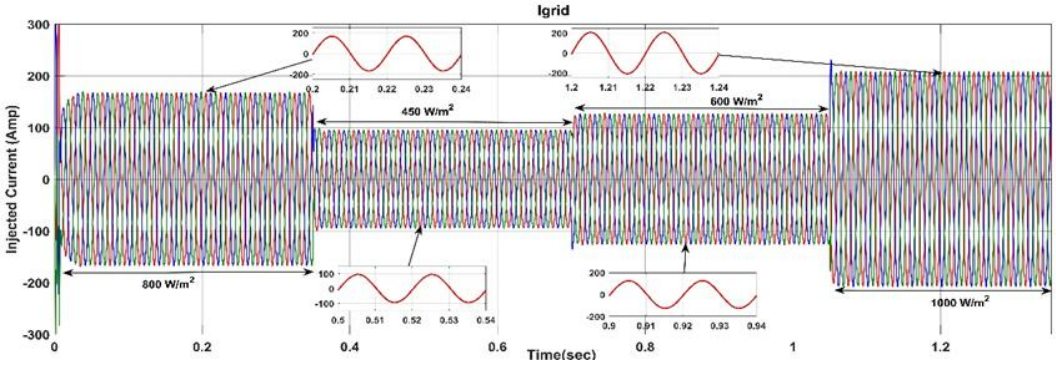

Figure 16. Three-phase injected grid current under varying solar irradiance levels using IC-MPPT

4. CONCLUSION

This study presents a detailed investigation into the effectiveness of the ANFIS-based MPPT approach to reduce THD in three-phase grid-connected PV systems, which demonstrates its role as a solution to both energy extraction and harmonic distortion. The ANFIS method maintained low THD values that were consistently lower than the IC-MPPT method, and the results from simulation at various irradiance levels from 450 W/m² to 1000 W/m² demonstrated that the intelligent ANFIS controller could provide superior power quality performance, with the lowest THD of 0.26% (40.9% lower than IC-MPPT) under optimal conditions1000 W/m², and a THD of 0.80% (28.6% lower than IC) at lower irradiance, 450 W/m². The ANFIS method also succeeded in maintaining a smooth and high-quality sinusoidal waveform of the injected grid current even during abrupt changes in solar irradiance. The low distortion rates confirmed the system's compliance with established standards like IEEE 519 and IEC 61000.

Although these results are compelling, the study highlights some methodological limitations to maintain academic awareness: The current comparative scope was limited to IC-MPPT and did not benchmark against other proven AI-based MPPT techniques (such as ANN or hybrid methods); key modeling factors, such as inverter switching losses and grid impedance, were not included in the simulation; and robustness testing under challenging external factors, such as noisy inputs or specific grid disturbances (voltage sags or asymmetrical faults), was not included in the analysis.

Future work should focus on quantifying key metrics such as MPPT tracking speed (convergence time) and cumulative energy harvested (energy yield) to fully validate the energy efficiency benefits of ANFIS. Subsequent studies must also incorporate rigorous robustness testing under simulated grid fault scenarios from the point of view of the application. The continued low THD achieved by ANFIS-MPPT strongly recommends its deployment in large PV plants, thus aligning the deployment strategy with the IEEE 519 and IEC 61000 compliance frameworks for improved grid-level energy quality. Future research may also explore the integration of ANFIS with other advanced control strategies in order to further optimize performance and adaptability to different operating environments.

FUNDING INFORMATION

No funding involved.

AUTHOR CONTRIBUTIONS STATEMENT

This journal uses the Contributor Roles Taxonomy (CRediT) to recognize individual author contributions, reduce authorship disputes, and facilitate collaboration.

Name of Author	C	M	So	Va	Fo	I	R	D	O	E	Vi	Su	P	Fu
Bouledroua Adel	✓	✓	✓	✓	✓	✓		✓	✓	✓			✓	✓
Mesbah Tarek		✓				✓		✓	✓	✓	✓	✓		✓
Kelaiaia Samia	✓		✓	✓			✓			✓	✓		✓	

C : **C**onceptualization
M : **M**ethodology
So : **So**ftware
Va : **Va**lidation
Fo : **Fo**rmal analysis
I : **I**nvestigation
R : **R**esources
D : **D**ata Curation
O : Writing - **O**riginal Draft
E : Writing - Review & **E**diting
Vi : **Vi**sualization
Su : **Su**pervision
P : **P**roject administration
Fu : **Fu**nding acquisition

CONFLICT OF INTEREST STATEMENT

Authors state no conflict of interest.

DATA AVAILABILITY

Data availability is not applicable to this paper as no new data were created or analyzed in this study.

REFERENCES

[1] G. Masson, A. Jäger-Waldau, I. Kaizuka, J. Lindahl, J. Donoso, and M. De L'Epine, "A snapshot of the global PV market," *Conference Record of the IEEE Photovoltaic Specialists Conference*, pp. 566–568, 2024, doi: 10.1109/PVSC57443.2024.10749131.

[2] O. O. Apeh, E. L. Meyer, and O. K. Overen, "Contributions of solar photovoltaic systems to environmental and socioeconomic aspects of national development—a review," *Energies*, vol. 15, no. 16, p. 5963, Aug. 2022, doi: 10.3390/en15165963.

[3] A. El Maghraoui, Y. Ledmaoui, O. Laayati, H. El Hadraoui, and A. Chebak, "Effect of large-scale PV integration onto existing electrical grid on harmonic generation and mitigation techniques," in *Proceedings - 2023 IEEE 5th Global Power, Energy and Communication Conference, GPECOM 2023*, Jun. 2023, pp. 294–299. doi: 10.1109/GPECOM58364.2023.10175736.

[4] L. Nogueira Pena Neto and J. Roberto Camacho, "Harmonic spectrum analysis at interconnection points between electrical power networks and photovoltaic systems via numerical simulation," in *International Symposium on Energy: Energy Transition, Green Hydrogen and Sustainable Industry - ISE 2023*, Dec. 2023. doi: 10.55592/ISE.2023.6894482.

[5] L. Scekic and S. Mujovic, "Long-term harmonic analysis of grid-connected photovoltaic systems," in *2022 20th International Conference on Harmonics & Quality of Power (ICHQP)*, May 2022, pp. 1–6. doi: 10.1109/ICHQP53011.2022.9808737.

[6] P. K. Dewangan and M. Singh, "Harmonic mitigation for enhancing grid-integrated photo voltaic system power quality: a review," *International Journal of Scientific Research in Engineering & Technology*, pp. 38–42, Mar. 2024, doi: 10.59256/ijsreat.20240402004.

[7] M. Z.-E. Masry, A. Mohammed, F. Amer, and R. Mubarak, "New hybrid MPPT technique including artificial intelligence and traditional techniques for extracting the global maximum power from partially shaded PV systems," *Sustainability*, vol. 15, no. 14, p. 10884, Jul. 2023, doi: 10.3390/su151410884.

[8] Ravinder Singh Maan, Alok Kumar Singh, and Ashish Raj, "Numerical simulation and mathematical analysis of meta heuristic MPPT system for solar photovoltaic applications under non-linear operational conditions," *Advances in Nonlinear Variational Inequalities*, vol. 27, no. 1, pp. 236–246, Mar. 2024, doi: 10.52783/anvi.v27.387.
[9] F. Alhaj Omar, "Comparative performance analysis of a feed-forward neural network-based MPPT for rapidly changing climatic conditions," *Konya Journal of Engineering Sciences*, vol. 11, no. 1, pp. 71–86, Mar. 2023, doi: 10.36306/konjes.1179030.
[10] A. Dawahdeh, H. Sharadga, and S. Kumar, "Novel MPPT controller augmented with neural network for use with photovoltaic systems experiencing rapid solar radiation changes," *Sustainability*, vol. 16, no. 3, p. 1021, Jan. 2024, doi: 10.3390/su16031021.
[11] M. Mohiuddin *et al*., "Mitigation of harmonics using novel sector-based switching pattern space vector pulse width modulation," *IEEE Access*, vol. 11, pp. 51465–51479, 2023, doi: 10.1109/ACCESS.2023.3278050.
[12] B. Adel, M. Tarek, and K. Samia, "Evaluation of pulse width modulation techniques to reduce total harmonic distortion in grid-connected PV systems," *International Journal of Power Electronics and Drive Systems (IJPEDS)*, vol. 16, no. 1, p. 564, Mar. 2025, doi: 10.11591/ijpeds.v16.i1.pp564-574.
[13] A. Abeysekara, C. Ekanayake, and H. Ma, "Analysing harmonic resonance behaviour of a grid-connected PV plant," in *2024 IEEE 34th Australasian Universities Power Engineering Conference (AUPEC)*, Nov. 2024, pp. 1–6. doi: 10.1109/AUPEC62273.2024.10807515.
[14] B. Pattanayak, S. Nanda, P. Kumari, and N. Kumar, "Advancement in techniques towards power quality improvement in Microgrid system: A comprehensive review," *E3S Web of Conferences*, vol. 540, p. 01016, Jun. 2024, doi: 10.1051/e3sconf/202454001016.
[15] T. Vu, D. Robinson, V. Gosbell, S. Elphick, J. David, and A. Johnston, "Harmonic challenges and practical solutions for transmission systems and renewable energy zones," in *2024 21st International Conference on Harmonics and Quality of Power (ICHQP)*, Oct. 2024, pp. 143–148. doi: 10.1109/ICHQP61174.2024.10768778.
[16] S. Bhattacharyya, D. S. Kumar P, S. Samanta, and S. Mishra, "Steady output and fast tracking MPPT (SOFT-MPPT) for P&O and InC algorithms," *IEEE Transactions on Sustainable Energy*, vol. 12, no. 1, pp. 293–302, Jan. 2021, doi: 10.1109/TSTE.2020.2991768.
[17] H. Alhusseini, M. Niroomand, and B. M. Dehkordi, "A fuzzy-based adaptive P&O MPPT algorithm for PV systems with fast tracking and low oscillations under rapidly irradiance change conditions," *IEEE Access*, vol. 12, pp. 84374–84386, 2024, doi: 10.1109/ACCESS.2024.3412848.
[18] M. R. Javed, A. Waleed, U. S. Virk, and S. Z. ul Hassan, "Comparison of the adaptive neural-fuzzy interface system (ANFIS) based solar maximum power point tracking (MPPT) with other solar mppt methods," in *2020 IEEE 23rd International Multitopic Conference (INMIC)*, Nov. 2020, pp. 1–5. doi: 10.1109/INMIC50486.2020.9318178.
[19] A. Taylor and S. M. Musa, "Evaluation of hybrid AI-based techniques for MPPT optimization," in *2022 International Conference on Green Energy, Computing and Sustainable Technology (GECOST)*, Oct. 2022, pp. 371–375. doi: 10.1109/GECOST55694.2022.10010563.
[20] D. K. Dash and P. K. Sadhu, "Emerging active power filtering techniques for grid-connected photovoltaic systems: a review of the latest developments and future directions," in *2023 IEEE 3rd International Conference on Smart Technologies for Power, Energy and Control (STPEC)*, Dec. 2023, pp. 1–6. doi: 10.1109/STPEC59253.2023.10430748.
[21] M. Bedoui, A. Berkani, K. Negadi, and F. Marignetti, "Power quality improvement in three-phase grid tied pv systems with 3-D SVPWM control active power filters," *Studies In Engineering and Exact Sciences*, vol. 5, no. 2, p. e9991, Oct. 2024, doi: 10.54021/seesv5n2-423.
[22] A. A. Al-Samawi and H. Trabelsi, "Power quality enhancement of PV system based on modified three-phase cascaded multilevel inverter," in *2022 19th International Multi-Conference on Systems, Signals & Devices (SSD)*, May 2022, pp. 339–346. doi: 10.1109/SSD54932.2022.9955937.
[23] N. Mishra, B. Singh, S. K. Yadav, and M. Tariq, "Power quality improvement in fifteen level PUC converter for solar PV grid-tied applications," *IEEE Transactions on Industry Applications*, vol. 59, no. 4, pp. 4264–4273, Jul. 2023, doi: 10.1109/TIA.2023.3260067.
[24] R. Rai, S. Saifi, S. Gupta, and P. Chittora, "Power quality improvement in grid-connected PV system with ANN-based control scheme," in *2024 IEEE Third International Conference on Power Electronics, Intelligent Control and Energy Systems (ICPEICES)*, Apr. 2024, pp. 476–481. doi: 10.1109/ICPEICES62430.2024.10719357.
[25] V. Yadav, B. Singh, and A. Verma, "Robust control for improving performance of grid-synchronized solar PV-BES-wind based microgrid," *Sustainable Energy Technologies and Assessments*, vol. 64, p. 103677, Apr. 2024, doi: 10.1016/j.seta.2024.103677.
[26] A. Tiwari, "Power quality enhancement in grid-connected PV systems with battery backup: A filterless control strategy," *Engineering Research Express*, vol. 7, no. 1, p. 015338, Mar. 2025, doi: 10.1088/2631-8695/adadc4.
[27] A. S. Al-Ezzi and M. N. M. Ansari, "Photovoltaic solar cells: a review," *Applied System Innovation*, vol. 5, no. 4, p. 67, Jul. 2022, doi: 10.3390/asi5040067.
[28] C.-M. Huang, S.-J. Chen, and S.-P. Yang, "Parameter estimation of a single-diode PV model using a hybrid charged system search algorithm," in *2020 IEEE 29th International Symposium on Industrial Electronics (ISIE)*, Jun. 2020, pp. 947–952. doi: 10.1109/ISIE45063.2020.9152526.
[29] C. Zhang, Y. Zhang, J. Su, T. Gu, and M. Yang, "Modeling and prediction of PV module performance under different operating conditions based on power-law I – V model," *IEEE Journal of Photovoltaics*, vol. 10, no. 6, pp. 1816–1827, Nov. 2020, doi: 10.1109/JPHOTOV.2020.3016607.
[30] P. S. M. Saad, M. Y. Bin Kasbudi, and H. Hashim, "I-V and P-V solar cell characteristics simulation for a single diode photovoltaic," in *2022 IEEE International Conference in Power Engineering Application (ICPEA)*, Mar. 2022, pp. 1–5. doi: 10.1109/ICPEA53519.2022.9744703.
[31] M. Khan, M. A. Raza, M. Faheem, S. A. Sarang, M. Panhwar, and T. A. Jumani, "Conventional and artificial intelligence based maximum power point tracking techniques for efficient solar power generation," *Engineering Reports*, vol. 6, no. 12, Dec. 2024, doi: 10.1002/eng2.12963.
[32] A. Hussien, A. Eltayesh, and H. M. El-Batsh, "Experimental and numerical investigation for PV cooling by forced convection," *Alexandria Engineering Journal*, vol. 64, pp. 427–440, Feb. 2023, doi: 10.1016/j.aej.2022.09.006.
[33] Y. Dhieb, M. Yaich, M. Bouzguenda, and M. Ghariani, "MPPT optimization using ant colony algorithm: solar PV applications," in *2022 IEEE 21st international Ccnference on Sciences and Techniques of Automatic Control and Computer Engineering (STA)*, Dec. 2022, pp. 503–507. doi: 10.1109/STA56120.2022.10019072.
[34] D. A. Pratama, F. Damsi, and M. S. Zarkasih, "Simulation of maximum power point tracking with fuzzy logic control method on solar panels using MATLAB," *Jurnal Teknologi Informasi dan Pendidikan*, vol. 17, no. 1, pp. 138–148, Jan. 2024, doi: 10.24036/jtip.v17i1.731.

[35] A. S. Putra, H. Afianti, and R. Watiasih, "Comparative analysis of solar charge controller performance between MPPT and PWM on solar panels," *JEECS (Journal of Electrical Engineering and Computer Sciences)*, vol. 7, no. 1, pp. 1197–1202, Jan. 2023, doi: 10.54732/jeecs.v7i1.217.
[36] D. A. Asoh, B. D. Noumsi, and E. N. Mbinkar, "Maximum power point tracking using the incremental conductance algorithm for PV systems operating in rapidly changing environmental conditions," *Smart Grid and Renewable Energy*, vol. 13, no. 05, pp. 89–108, 2022, doi: 10.4236/sgre.2022.135006.
[37] A. Asnil, R. Nazir, K. Krismadinata, and M. N. Sonni, "Performance analysis of an incremental conductance MPPT algorithm for photovoltaic systems under rapid irradiance changes," *TEM Journal*, vol. 13, no. 2, pp. 1087–1094, May 2024, doi: 10.18421/TEM132-23.
[38] M. Ahmad, A. Numan, and D. Mahmood, "A comparative study of perturb and observe (P&O) and incremental conductance (INC) PV MPPT techniques at different radiation and temperature conditions," *Engineering and Technology Journal*, vol. 40, no. 2, pp. 376–385, Feb. 2022, doi: 10.30684/etj.v40i2.2189.
[39] Bachar Meryem, Naddami Ahmed, and Fahli Ahmed, "Simulation and implementation of a modified ANFIS MPPT technique," *Advances in Technology Innovation*, Aug. 2020, doi: 10.46604/aiti.2020.4987.
[40] S. Lakshminarayanan, H. D. Kattimani, and P. A. Athavale, "An MPPT charge controller for solar PV installations using the incremental conductance method," in *2025 International Conference on Computing for Sustainability and Intelligent Future (COMP-SIF)*, Mar. 2025, pp. 1–6. doi: 10.1109/COMP-SIF65618.2025.10969962.
[41] A. Kumar, M. Rizwan, and U. Nangia, "Development of ANFIS-based algorithm for MPPT controller for standalone photovoltaic system," *International Journal of Advanced Intelligence Paradigms*, vol. 18, no. 2, p. 247, 2021, doi: 10.1504/IJAIP.2021.112906.
[42] R. T. Moyo, P. Y. Tabakov, and S. Moyo, "Design and modeling of the ANFIS-Based MPPT controller for a solar photovoltaic system," *Journal of Solar Energy Engineering*, vol. 143, no. 4, Aug. 2021, doi: 10.1115/1.4048882.

BIOGRAPHIES OF AUTHORS

Bouledroua Adel was born in Annaba (Algeria) on March 4, 1982. He graduated from the University of Badji Mokhtar, Department of Electromechanical Engineering (Algeria), in 2005. He received the degree of Magister in electromechanical Engineering from the University of Badji Mokhtar Annaba in 2008, and he is currently pursuing his Ph.D. from Badji Mokhtar University. His research interests include the field of renewable energy, photovoltaic power systems, wind applications, power electronics, motor drives, and artificial intelligence. He can be contacted at email: adel.bouledroua@univ-annaba.dz.

Mesbah Tarek received his B.E. degree, Master and Ph.D. Degrees in Electrical Engineering from Badji Mokhtar University of Annaba, Algeria. Currently, he is a professor at the Badji Mokhtar University of Annaba. His research interests include the field of power grid, smart grid, power system optimization, and renewable energy. He can be contacted at email: tarek.mesbah@univ-annaba.dz.

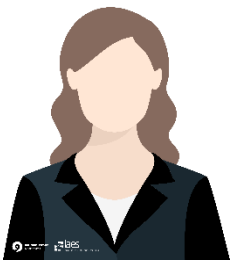

Kelaiaia Samia received her B.E. degree, master and Ph.D. degree in electrical engineering from Badji Mokhtar University of Annaba, Algeria. Currently, she is an assistant professor at the Badji Mokhtar University of Annaba. Her current research interests include power electronics, renewable energy, and renewable energy integration to the power grid. She can be contacted at email: samia.kelaiaia@univ-annaba.dz.